PROC. OF JSCE
No. 337, September 1983

FUNDAMENTAL STUDY ON UNSTEADY FLOW AROUND UNDERGROUND CAVERN IN UNCONFINED GROUNDWATER

By Kuniaki SATO and Masato IIZAWA***

1. INTRODUCTION

Until now, many underground caverns and tunnels have been constructed for various purposes, such as electric power stations, oil store caverns and railroad tunnels. Knowledge of reliable informations concerning with groundwater movement and discharge is indispensable to the excavation works of tunnels and caverns. Hydraulic problems of tunnel are mainly an extraordinary flooding, the tunnel discharge, the groundwater withdrawal and an unexpected pressure acting on tunnel supports. On the other hand, those of caverns depend on the utility, the purposes and the cavern scale. For the case of cavern, it is particularly important to clarify the degression mechanism of discharge into cavern with time and withdrawal process of free surface in unconfined aquifer.

In many cases, both caverns and tunnels are excavated in rock masses. However, it is inevitably necessary to introduce suitable models of rock aquifer in order to study the behavior of flow with simplified conditions. Most existing studies have dealt with the steady flow of drain hole and the tunnel having a round form section in a horizontally uniform stratum. Dagan (1964)[1] analyzed the steady flow around the drain hole with constant infiltration at ground surface, and Polubarinova-Kochina (1962)[2] derived a solution of unsteady flow by a method of perturbation approximation in unconfined uniform stratum of infinite thickness. Sato and Otabe (1978)[3] gave an analytic solution of unconfined flow having a circular grouting zone around the tunnel in a horizontally uniform layer. On the other hand, Ishii et al. (1977)[4] and Takahashi (1962)[5] examined the seepage characters of railway tunnels by using a number of field measurement data in Japan. In recent years, Chishaki (1979)[6] and Komata et al. (1979)[7] analyzed numerically the groundwater motion around the tunnel and the cavern by the finite element method, and Tanaka and Aki (1979)[8] calculated the groundwater movement around the oil store cavern by the application of finite difference method in an unconfined horizontal stratum. Most studies mentioned above deal with steady groundwater motion, and analyze steady discharge into tunnel or drain. However, taking the deep groundwater behavior into consideration, it is required to examine the unsteady behavior of groundwater around a large scale cavern as compared with the drain hole or tunnel, since the local dynamics of water such as pressure change and free surface being adjacent to the wall of cavern may become important.

Then, this paper aims at the study of the fundamental characteristics and the motion of unsteady flow by means of the numeric computation of governing equation by the finite difference method around the large cavern in unconfined groundwater. In addition, their computed results are discussed by using the experimental ones obtained from Hele-Shaw apparatus.

2. NUMERICAL ANALYSIS OF FLOW

It is difficult to obtain rigorous solution of unsteady flow around the cavern from the governing equation and some practical conditions. Free surface falls gradually from the early stage of water level, and it reaches to the upside wall of cavern with time elapsed. The free surface will become a steady state around the cavern after time elapsed enough. Similarly, the discharge into cavern decreases with time. In a such process of lowering free surface, three

* Member of JSCE, Dr. Eng. Associate Professor, Hydroscience and Geotechnology Laboratory, Faculty of Engineering, Saitama University, Urawa, Japan

** Member of JSCE, M. S., Eng. Electric Power Development Co., Ltd., Tokyo, Japan

hydraulic stages of flow can be observed in the vertically two-dimensional stratum. At the first stage, the free surface falls rapidly from an initially flat level, and at the second stage, the seepage-out surface is the inside wall of cavern until the flow domain becomes steady state at third stage. The following analysis intends to clarify the unsteady behaviors with the moving free surface and the change of discharge into cavern with time by using numerical computations in the vertical stratum. Then, several characteristics of flow will be compared with the experimental results.

(1) Governing Equation and Boundary Conditions

We consider a vertical two-dimensional stratum having a cavern in it, as shown in **Fig. 1**. It is assumed that the cavern has a rectangular section, the stratum is horizontal with the length L, and the free surface has a constant depth at the initial stage. The flow domain is symmetric with the vertical axis passing through the center of cavern.

The basic equation used in this analysis is derived from the continuity equation and Darcy's law as,

$$\frac{\partial}{\partial x}\left(k_x\frac{\partial h}{\partial x}\right)+\frac{\partial}{\partial z}\left(k_z\frac{\partial h}{\partial z}\right)=n_0\frac{\partial h}{\partial t} \quad \cdots\cdots(1)$$

in which h=piezometric head, x, z=horizontal and vertical axes, k_x, k_y=permeabilities in the x- and z-directions, respectively, n_0=effective porosity, and t=time. In case of steady flow through an isotropic and homogeneous stratum, Eq. (1) becomes,

$$\nabla^2 h=0 \quad \cdots\cdots(2)$$

in which ∇^2=Laplacian operator.

Groundwater motion is known by solving Eq. (1) under given conditions. However, for the sake of convenience of numerical computation the method of gradual succession of stationary states based on Eq. (2) is used in the following analysis. The kinematic condition at the free surface is written by putting $z=\eta(x, t)$ as,

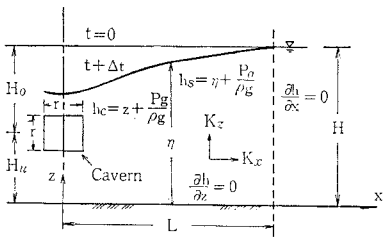

Fig. 1 Model of cavern and flow conditions.

$$\frac{D\eta}{Dt}=\frac{\partial\eta}{\partial t}+u_s\frac{\partial\eta}{\partial x}=w_s \quad \cdots\cdots(3)$$

where u_s, w_s=velocity components in the x- and z-axes at free surface, respectively.

On the other hand, these u_s and w_s can be written as,

$$u_s=-\frac{k_x}{n_0}\frac{\partial h}{\partial x}\Big]_{z=\eta}, \qquad w_s=-\frac{k_z}{n_0}\frac{\partial h}{\partial z}\Big]_{z=\eta}$$

where $]_{z=\eta}$=values of u_s and w_s at free surface. Therefore, the relationship between u_s and w_s can be written by

$$u_s=-\frac{k_x}{n_0}\frac{\partial h_s}{\partial x}-\frac{k_x}{k_z}\frac{\partial\eta}{\partial x}w_s \quad \cdots\cdots(4)$$

if the piezometric head h_s is defined by $h_s(x, t)=h]_{z=\eta}=h(x, \eta(x, t), t)$.

Boundary conditions to be imposed are:

$$\frac{\partial h}{\partial x}\Big]_{x\to L}=0 \qquad \eta=0 \text{ for } L\gg r: \quad \cdots\cdots(5)$$

$$\frac{\partial h}{\partial z}\Big]_{z=0}=0: \quad \text{at impermeable bottom,} \quad \cdots\cdots(6)$$

$$h_s=\eta+p_a/\rho g: \quad \text{at free surface,} \quad \cdots\cdots(7)$$

$$h_c=z+p_g/\rho g: \quad \text{at wall of cavern,} \quad \cdots\cdots(8)$$

in which p_a=atmospheric pressure, p_g=gas pressure in cavern, ρ=density of fluid and h_c=piezometric head at wall of cavern. To analyze the groundwater movement around the cavern the governing equation given by Eq. (1) must be solved under the boundary conditions written by Eqs. (5) through (8), in addition to the kinematic condition at free surface.

Flow rate into the cavern q_c can be found by,

$$q_c=-k_n\frac{\partial h}{\partial n}: \quad \text{at wall of cavern,} \quad \cdots\cdots(9)$$

where k_n=permeability normal to wall, taken as the outer direction plus, and n is the normal direction to wall.

(2) Finite Difference Schemes of Governing Equation and Boundary Conditions

To obtain the numerical solution of flow as given by **Fig. 1**, the appropriate schemes of computation are needed for the governing equation, kinematic condition and boundary conditions. The finite difference schemes proposed by Tanaka and Aki (1979) are mainly used in the following computations. For the sake of computational convenience, the so-called "method of gradual succession of stationary states" is adopted in half domain of flow in **Fig. 1**.

For the steady flow the governing equation can be written by the Over-Relaxation Method as,

$$^{m+1}h_{ij}^{n+1}={}^{m}h_{ij}^{n+1}+\kappa(\tilde{h}_{ij}^{n+1}-{}^{m}h_{ij}^{n+1}) \quad \cdots\cdots(10)$$

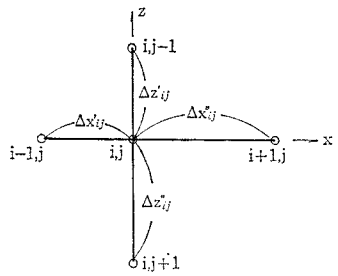

(a) Non-uniform mesh points in flow domain

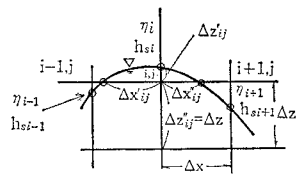

(b) Finite difference meshes near free surface

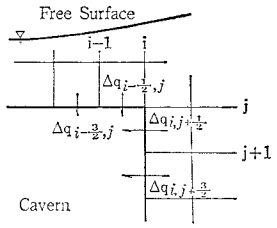

(c) Numerical determination of flow rate into cavern in case of submerged flow

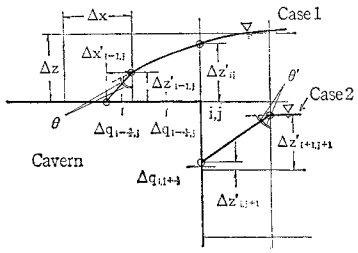

(d) Numerical determination of flow rate into cavern in case of non-submerged flow having seepage-out

Fig. 2 Finite difference schemes of numerical analyses.

where κ=relaxation factor, and i, j=mesh number of finite difference scheme ($i, j=1, 2, 3, \cdots$). In Eq. (10) $\tilde{h}_{ij}^{n+1}$ can be written from **Fig. 2** (a) by,

$$\tilde{h}_{ij}^{n+1}=\frac{1}{k_x\Delta z'_{ij}\Delta z''_{ij}+k_z\Delta x'_{ij}\Delta x''_{ij}}\left\{k_x\Delta z'_{ij}\Delta z''_{ij}\times\frac{\Delta x''^{\,m+1}_{ij}h^{n+1}_{i-1,j}+\Delta x'^{\,m}_{ij}h^{n+1}_{i+1,j}}{\Delta x'_{ij}+\Delta x''_{ij}}+k_z\Delta x'_{ij}\Delta x''_{ij}\times\frac{\Delta z''^{\,m+1}_{ij}h^{n+1}_{i,j-1}+\Delta z'^{\,m}_{ij}h^{n+1}_{i,j+1}}{\Delta z'_{ij}+\Delta z''_{ij}}\right\} \quad \cdots\cdots(11)$$

in which the numerical computation must be repeated until the following condition is satisfied,

$$\left|\frac{\tilde{h}_{ij}^{n+1}-{}^{m}h_{ij}^{n+1}}{{}^{m+1}h_{ij}^{n+1}}\right|<\varepsilon \quad \cdots\cdots(12)$$

where, ε is a convergence value 10^{-4}, and m: the repeat number of computations.

The kinematic condition at free surface can be written by Lax-Wendroff scheme as,

$$\eta_i^{n+1}=\eta_i^n+\left(w_{si}^n-u_{si}^n\frac{\eta_{i+(1/2)}^{n+(1/2)}-\eta_{i-(1/2)}^{n+(1/2)}}{\Delta x}\right)\Delta t \quad \cdots(13)$$

from Eq. (3), and

$$\eta_{i+(1/2)}^{n+(1/2)}=\frac{\eta_{i+1}^n+\eta_i^n}{2}+\left(\frac{w_{si+1}^n+w_{si}^n}{2}-\frac{u_{si+1}^n+u_{si}^n}{2}\frac{\eta_{i+1}^n-\eta_i^n}{\Delta x}\right)\frac{\Delta t}{2},$$

$$\eta_{i-(1/2)}^{n+(1/2)}=\frac{\eta_i^n+\eta_{i-1}^n}{2}+\left(\frac{w_{si}^n+w_{si-1}^n}{2}-\frac{u_{si}^n+u_{si-1}^n}{2}\frac{\eta_i^n-\eta_{i-1}^n}{\Delta x}\right)\frac{\Delta t}{2}.$$

In Eq. (13) the stability condition of computation becomes,

$$\frac{\Delta x_{ij}}{\Delta t}\geqq|u_{si}^n| \quad \cdots\cdots(14)$$

Here, referring to **Fig. 2** (b), u_{si}^n and w_{si}^n are written by, respectively,

$$\left.\begin{aligned}u_{si}^n&=\frac{k_x}{2n_0\Delta x_{ij}}\left\{h_{si-1}^n-h_{si+1}^n+\frac{n_0}{k_z}w_{si}^n(\eta_{i-1}^n-\eta_{i+1}^n)\right\}\\ w_{si}^n&=\frac{k_z}{n_0}\frac{h_{ij}^n-h_{ij}^n}{\Delta z'_{ij}}.\end{aligned}\right\}$$

Flow rate into the cavern can be computed from Eq. (9) as,

$$\left.\begin{aligned}\Delta q_{i-(1/2),j}&=k_z\frac{h_{i-1,j-1}+h_{i,j-1}-h_{i-1,j}-h_{ij}}{2\Delta z}\Delta x\\ \Delta q_{i,j+(1/2)}&=k_x\frac{h_{i+1,j}+h_{i+1,j+1}-h_{ij}-h_{i,j+1}}{2\Delta x}\Delta z.\end{aligned}\right\} \quad \cdots\cdots(15)$$

by referring **Fig. 2** (c).

On the other hand, two different schemes on the basis of Dupuit's formula are used for determining the flow rate after the free surface is in contact with the cavern wall. Referring to Case-1 and Case-2 in **Fig. 2** (d), each scheme is obtained as follows:

$$\Delta q_{i-(3/2),j}=k_z\frac{h_{si-1}-h_{i-1,j}}{2\Delta z'_{i-1,j}}\Delta x'_{i-1,j}, \quad \cdots\cdots(16\cdot a)$$

$$\Delta q_{i-(1/2),j}=k_z\frac{1}{2}\left\{\frac{h_{si-1}-h_{i-1,j}}{\Delta z'_{i-1,j}}+\frac{h_{si}-h_{ij}}{\Delta z'_{ij}}\right\}\Delta x_{ij}, \quad \cdots\cdots(16\cdot b)$$

$$\Delta q_{i,j+1}=k_z\frac{h_{si+1}+h_{i+1,j+1}-h_{si}-h_{i,j+1}}{2\Delta x_{i+1,j+1}}\times\frac{\Delta z'_{i,j+1}+\Delta z'_{i+1,j+1}}{2}, \quad \cdots\cdots(17)$$

Determining the seepage-out point of free surface at the wall of cavern, the following assumption is adopted: the free surface refracts downwards with one half angle of tangent on nearest vertical mesh (cf. **Fig. 2** (d)). This method for determining the seepage-out point is convenient, and it was proposed by Tanaka and Aki (1979).

Other boundary conditions corresponding to Eqs. (5), (6), (7) and (8) are written by, respectively,

$$\eta_i^{n+1}=\eta_i^n+\frac{p_a}{\rho g}:\quad \eta_{ij}^{n+1}=\eta_i^n \quad \text{for } L\gg r \cdots\cdots(18)$$

$$\frac{h_{i,j+1}-h_{i,j-1}}{2\Delta z}=0:\quad \text{at impermeable bottom,} \cdots\cdots(19)$$

$$h_{si}=\eta_i+p_a/\rho g,\ h_{si}=\eta_i:\quad \text{at free surface,} \cdots\cdots(20)$$

$$h_{ij}=z_{ij}+p_g/\rho g:\quad \text{at wall of cavern.} \cdots\cdots(21)$$

(3) Computation Procedure

By using a set of Eqs. (10)~(21), the required solution of flow around the cavern can be obtained for the initial and boundary conditions. Computational procedure will be summarized in the following: ① the piezometric head in groundwater aquifer is computed by Eqs. (10), (11) and (12) for the initial condition under the boundary conditions of Eqs. (18)~(21), ② the flow rate into the cavern can be given by Eqs. (15), (16) and (17) from the piezometric head distribution at that very instant, and the free surface change is computed from the water particle velocity at the free surface, ③ new piezometric head is found at free surface and in aquifer after the time elapsed. The computational procedure is repeated for time steps as shown in **Fig. 3**. The free surface at initial stage is horizontal in whole aquifer, and it is constant at $x=L$. For the sake of simplicity, the gas pressure p_g in cavern is regarded as the atmospheric one p_a in Eq. (21), and the aquifer is uniform: $k_x=k_z$.

For all computations three different intervals of mesh were used for the sake of accuracy improvement. Flow domain is covered by mesh intervals with $\Delta x_1=0.2L/i_1$, $i_1=16$ for $0<x\leqq 0.2L$, $\Delta x_2=0.3L/i_2$, $i_2=12$ for $0.2L<x\leqq 0.5L$ and $\Delta x_3=0.5L/i_3$, $i_3=10$ for $0.5L<x\leqq L$.

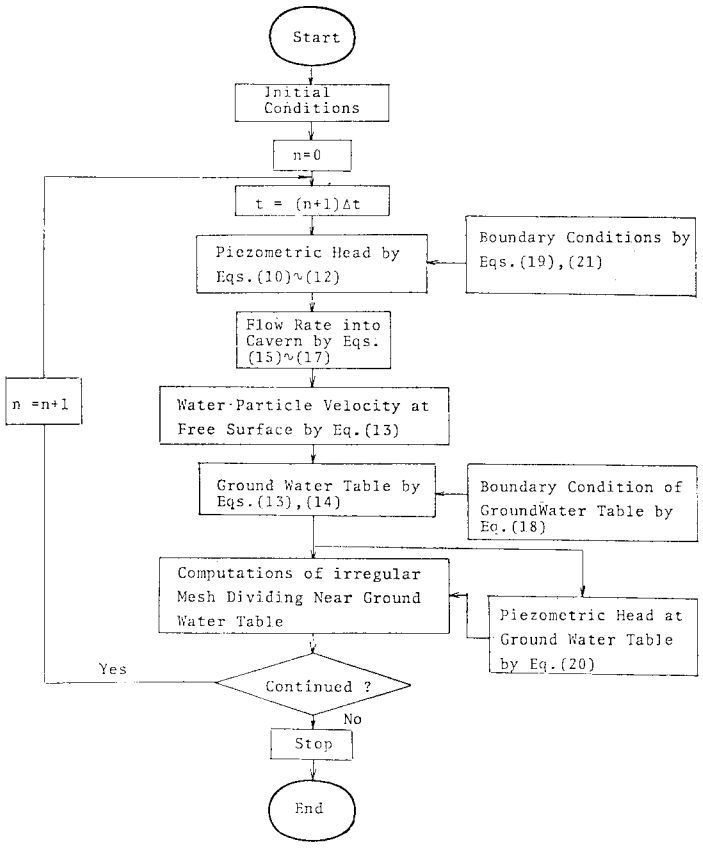

Fig. 3 Computational flow of groundwater.

3. EXPERIMENTAL APPARATUS AND CASES

In order to examine the flow characters around the cavern, experiments were carried out by Hele-Shaw model as shown in **Fig. 4**. This model is made from two transparent plates, and it is 102 cm in horizontal length and 30 cm in height. Viscous oil flows in a parallel interstice of 0.2 cm in thickness, and there is a cavern model of rectangular section $(2.5)^2$ cm^2 at the center of aquifer model. Kinematic viscosity of fluid is 2.840 cm^2/s, and the specific weight is 0.880 at temperature 19°C. Permeability is 1.150 cm/s. All experiments were carried out in a constant temperature room.

Experimental procedure is explained in the following manner. Prior to the experiment, the cavern model was blocked by a blockage metal (cf. **Fig. 5**), and the aquifer was filled with viscous oil under the same level of over-flow tanks. Then, the blockage metal was removed almost instantaneously, and the photographic observation of falling free surface was started. Flow rate into the cavern was measured by a graduated cylinder with time. A few seconds of time lag are unavoidable at an early stage of experiment, since the flux of seepage-out fluid from the cavern drops directly into the graduated cylinder.

Experimental cases were shown in **Table 1**. The water depth in stratum varies from 0.15 m to 0.25 m for H_u=0.1 m, L=0.51 m, r=0.025 m, and $k=k_x=k_z=0.0115$ m/s.

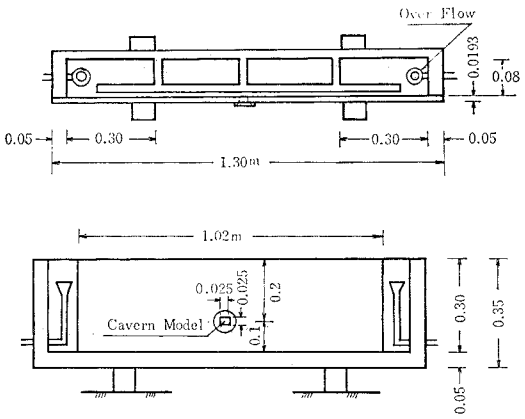

Fig. 4 Experimental apparatus.

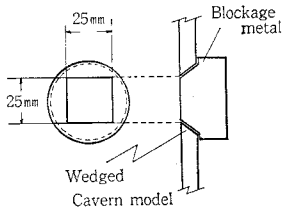

Fig. 5 Detail of experimental device for using blockage metal.

4. RESULTS OF NUMERICAL COMPUTATIONS AND EXPERIMENTS

Here, unsteady motion of free surface and change of flow rate with time are examined as compared the numerical solutions with experimental results for given conditions as shown in **Table 1**. **Fig. 6** shows the free surface curves of Run-1 at times of 0, 4, 8, 16, 20 and 60 seconds in half vertical section. Free surface falls gradually with time, and the draw-down velocity is maximum at the top of cavern. Numerical solution agrees closely with the experimental result as a whole. Relationship between non-dimensional time $T=kt/n_0r$ and non-dimensional draw-down head $\Delta h/H$ at the top of cavern is presented by **Fig. 7** in case of Run-1. It seems that the linear relation may be concluded. Chishaki (1977) pointed out that the draw-down head Δh is subjected to an exponential function of time t, in consequence of the numerical computations by the finite element method. For reference of fitness, the exponential function is shown by the dotted line in **Fig. 7**. Furthermore, the distribution of velocity vectors can be computed as in

Table 1 Experimental conditions (Notations are the same with in **Fig. 1**).

Case	H (m)	H_0 (m)	Hu (m)	L (m)	r (m)	k_x (m/s)	k_z (m/s)
Run-1	0.250	0.150	0.100	0.510	0.025	1.150×10^{-2}	1.150×10^{-2}
Run-2	0.225	0.125	0.100	0.510	0.025	1.150×10^{-2}	1.150×10^{-2}
Run-3	0.200	0.100	0.100	0.510	0.025	1.150×10^{-2}	1.150×10^{-2}
Run-4	0.175	0.075	0.100	0.510	0.025	1.150×10^{-2}	1.150×10^{-2}
Run-5	0.150	0.05	0.100	0.510	0.025	1.150×10^{-2}	1.150×10^{-2}

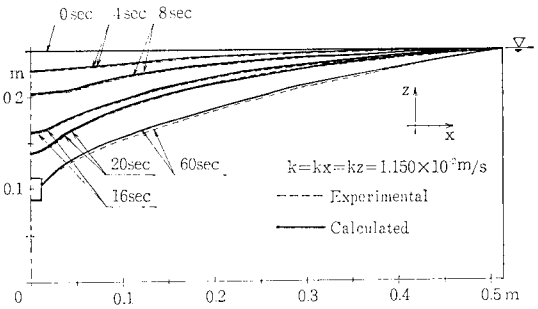

Fig. 6 Falling free surface in case of Run-1.

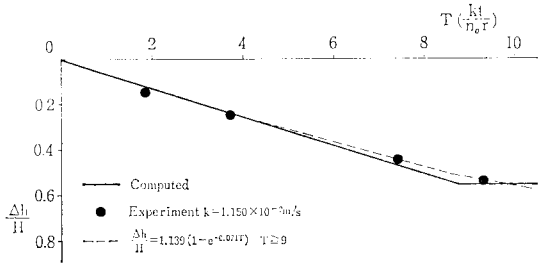

Fig. 7 Relationship between $T=kt/n_0r$ and $\Delta h/H$ in case of Run-1.

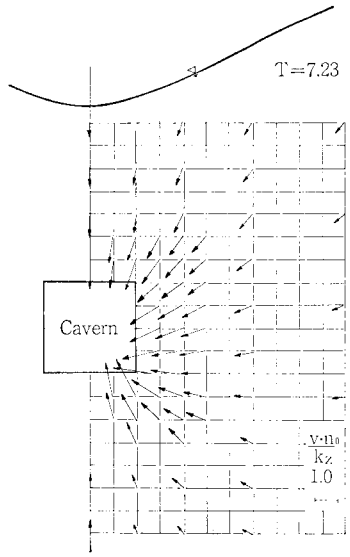

Fig. 8 Computed velocity vectors around cavern in case of Run-1.

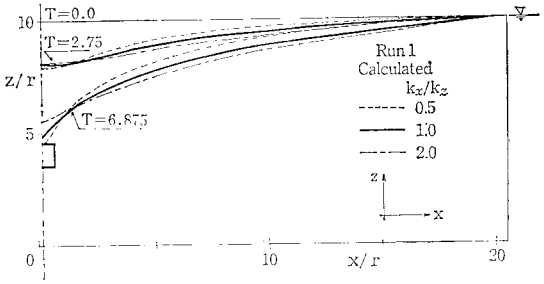

Fig. 9 Falling free surfaces computed for anisotropic permeabilities.

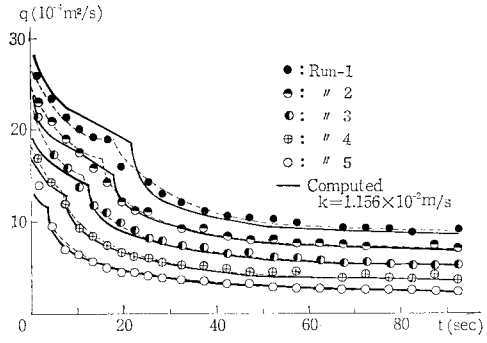

Fig. 10 Degression curves of flow rate for all experiments.

Fig. 8 for Run-1. It can be found that the flow toward the cavern occurs radially as a whole, and the velocity vectors become large around the right side corner of cavern for non-dimensional time $T=7.23$. Needless to say, since this field of velocity changes with time T, the magnitude of vectors diminishes as the discharge into cavern decreases with time. Next, in order to examine the anisotropic effect of aquifer, the non-dimensional free surface curves are computed in case of the permeability ratios of $k_x/k_z=0.5$, 1.0 and 2.0 at non-dimensional times $T=k_zt/n_0r=0.0$, 2.75 and 6.875 in **Fig. 9**. The results that indicate the draw-down speed at the top of cavern become larger as the ratio k_x/k_z decreases, and are closely related with anisotropic permeability of aquifer.

Flow rate changes with time are shown in **Fig. 10** for all cases. Each degression curve of flow rate has a characteristic inflection point at a time in both experimental and numeric results. The inflection point is caused by the fact that the free surface at the top of cavern will be contact with the cavern wall. Time of the point is somewhat different between numerical and experimental results, since unavoidable time lag occurs at the beginning of flow rate measurement. In order to clarify the hydraulic cause for the appearance of inflection point, three flow rate components are computed by using non-dimensional flow rate q/kr and the time kt/n_0r in **Fig. 11**, in which Q_1, Q_2 and Q_3 are downward, sideward and upward flow rates, respectively. It

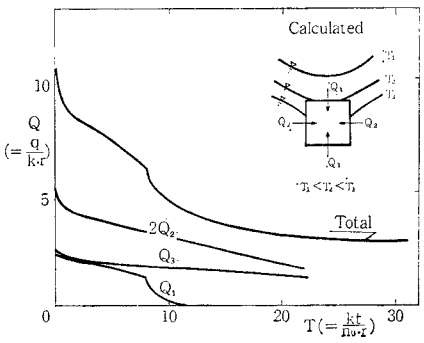

Fig. 11 Flow rate components computed for Run-1.

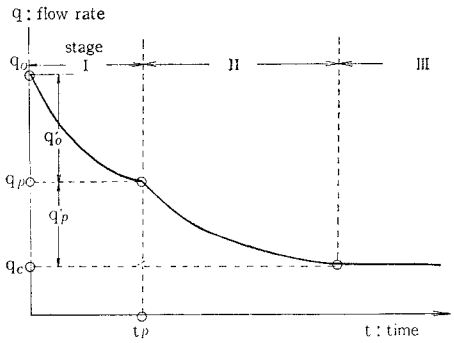

Fig. 12 Schematic presentation of degression curve.

is found from **Fig. 11** that the inflection point is originated in the downward flow rate component Q_1, since $2Q_2$ and Q_3 decrease gradually with time. Strictly speaking, dQ_2/dt may slightly change immediately after $Q_1=0$, but it is negligibly small. Total flow rate Q is $Q_1+2Q_2+Q_3$. Then, the schematic presentation of degression curve can be proposed as shown in **Fig. 12.** Three degression stages can be defined on the basis of pattern of curve. The first stage is abruptly decreasing stage, the second is gradually decreasing one and the third is constant one at time elapsed enough. To formulate the degression curve in the sense of engineering practice, the following equations can be appllied,

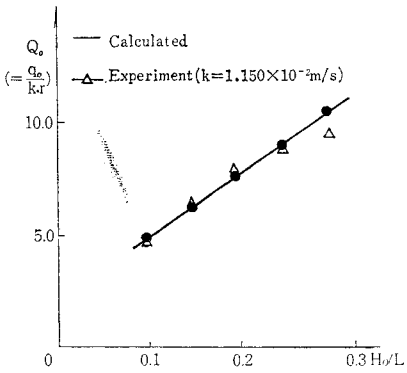

Fig. 13 Relationship between initial flow rate Q_0 and hydraulic gradient H_0/L for all cases.

$$q = q_0' (e^{-at} - e^{-at_p}) + q_p \,,$$
$$\text{for stage I } (0 \leqq t < t_p), \quad \cdots\cdots\cdots\cdots (22)$$
$$q = q_p' e^{-a'(t-t_p)} + q_c \,,$$
$$\text{for stage II, III, } (t_p \leqq t < \infty) \quad \cdots\cdots (23)$$

where q_0, q_p, q_c=flow rate at times $t=0$, $t=t_p$, $t=\infty$, respectively. In **Fig. 10**, the quantities obtained from experiments in Eqs. (22) and (23) are summarized as in **Table 2**. Degression curves of flow rate by those quantities for each experimental case are shown by dotted lines in **Fig. 10.** Degression rates a and a' of each curve are not constant, and in particular, the degression rate a changes with H_0/L. Namely, the value a increases as H_0/L decreases because $(H-H_0)/L$ is constant for all experiments. As a result of the experiments and numerical computations, the flow rate decreases abruptly in stage I with large degression rate a as H_0/L becomes small, and on the other hand, it decreases slowly in stage II.

Relationship between initial flow rate $q_0 = q_p + q_0'$ and hydraulic gradient H_0/L are given as shown in **Fig. 13**, as compared the numerical results with experimental ones. Both results

Table 2 Experimental quantities in Eqs. (22) and (23).

Experiment Cases	q_0' ($\times 10^{-4}$ m²/s)	q_p ($\times 10^{-4}$ m²/s)	a	q_p' ($\times 10^{-4}$ m²/s)	q_c ($\times 10^{-4}$ m²/s)	a'	t_p (s)
Run-1	8.0	19.0	0.166	10.0	9.0	0.075	18.0
Run-2	8.0	17.0	0.173	10.0	7.0	0.077	15.0
Run-3	8.0	15.0	0.277	9.8	5.2	0.081	12.0
Run-4	5.7	13.5	0.445	10.0	3.5	0.073	6.5
Run-5	—	—	—	7.8	2.3	0.058	4.5

show a slight discrepancy because of measuring error at the beginning of experiment: i.e., by unavoidable error originated from time lag. With respect to the hydraulic effect due to different section of cavern, flow rate and free surface were investigated by a rectangular section and a circular one with same area. However, it can not be found to discriminate the significant difference between both sections from the experiments, since the size of cavern is small ($r=2.5$ cm) and some measuring difficulties involve. Chishaki (1979) has pointed out the effect due to the different section of undersea tunnel by the finite element method for three sections of circular, horseshoe and rectangular shapes having same height and width. According to his computation, the flow rate increments are 3.9% for horseshoe shape and 7.3% for rectangular one as compared with that of circular section under the conditions of sea depth 20 m, tunnel diameter 10 m, aquifer thickness 40 m, horizontal length of aquifer 120 m and tunnel height from impervious bed 20 m, though the sectional area increments are 13.6% for horseshoe shape and 27.3% for rectangular one. Hydraulic effect due to the different section of cavern is not so large except the circumference around the cavern, provided that the aquifer scale is enough large as compared with the cavern size.

5. CONCLUSION

Fundamental characteristics and movement of unsteady groundwater around the cavern were examined for unconfined aquifer by virtue of the numerical computation of governing equation and the experiments by using Hele-Shaw apparatus. Particularly, the author paid attention to the degression mechanism of seepage flow rate into the cavern and the withdrawal process of free surface with time after the excavation of cavern. By this study, the following results are concluded.

Degression curve of seepage flow rate with time can be expressed approximately by exponential decreasing function of time, and three degression stages including abruptly decreasing stage and constant stage at time elapsed enough were found in both experiment and numerical solution. Flow rate is not so related with sectional form of cavern, and the flow velocity vectors are subjected to the influence of cavern form in only vicinity of cavern. Draw-down free surface and flow rate are much affected by the anisotropy of groundwater aquifer. In addition, possibility of application of finite difference scheme in this study is confirmed by experiments.

Finally, this joint study was carried out at Saitama University during the period when the junior author M. Iizawa was a graduate student.

6. NOTATIONS

The following symbols are used in this paper:

g = Acceleration of gravity
h = Piezometric head, $i,j=1, 2, 3, \cdots$
k_x, k_z, k_n = Permeabilities in x, z and normal directions
n, m = Numbers of finite difference mesh
n_0 = Effective porosity
p_a, p_g = Atmospheric and gas pressures
q, Q = Flow rate, x, z = Coordinates
Δx Δz = Finite difference in x and z directions
t = Time, D/Dt = Euler's operator
u, w = Velocity components in x and z directions, ρ = Fluid density
η = Piezometric head at free surface
ε = Small number, κ = Relaxation factor

REFERENCES

1) Dagan, G.: Spacing of drains by approximate method, Proc. ASCE, Irri. pp. 41~66, 1964.
2) Polubarinova-Kochina, P. Ya: Theory of Ground Water Movement, Translated by J. M. Roger de Wiest, Princeton Univ. Press, 1962.
3) Sato, K. and J. Otabe: Analysis of seepage-free surface around the tunnel, Proc. the 22nd Japanese Conference on Hydraulics, JSCE, 1978 (in Japanese).
4) Ishii, M. and H. Sakuma: Geomorphological and geological classifications of tunnel water—From the permanent tunnel water surveys at Japanese main railway tunnels—, Railway Technical Research Report, No. 1041, 1977 (in Japanese).
5) Takahashi, H.: Geological conception for tunnel water—Pre-estimating method for amount of tunnel water—, Railway Technical Research Report, No. 279, 1962 (in Japanese).
6) Chishaki, T.: Fundamental study on tunnel water, Rept. the Grant-in-Aid for Scientific Research, Japanese Ministry of Sci. and Culture, 1979 (in Japanese).
7) Komata, H., K. Nakagawa, Y. Kitahara and M. Hayashi: Study on development in technique of unlined underground storage of petroleum, Rept. Central Inst. Elec. Power Industry, No. 378028, 1979 (in Japanese).
8) Tanaka, N. and S. Aki: Studies on technical developments for unlined underground storage of fuel, Rept. Central Inst. Elec. Power Industry, No. 379006, 1979 (in Japanese).

(*Received October 6, 1982*)

和文要旨

不被圧地山における地下空洞周辺の非定常流に関する基礎研究

（佐藤邦明／飯沢雅人）

論文報告集，第337号，1983年9月

地下発電所，燃料貯蔵，核燃料廃棄などの目的から，岩盤地下空洞にかかわる諸問題が注目されている．中でも地下水に関する研究は問題の要となるため，強く求められている．このような背景にあって，本論は，空洞周辺の非定常地下水流に着目し，基礎的な流れの性質を明らかにしようとしたものであり，ヘル・ショウ実験と数値解析の両面から，湧水てい減特性，および地山の異方性と自由水面の低下機構を明らかにしている．

地下空洞にかかわる地下水流がトンネルや暗きょの流れと違う点は空洞寸法が対象地山スケールに比べ必ずしも小さくなく，空洞掘削に伴う地下水位，湧水の非定常プロセスが重要になることであり，特に，空洞への湧水の非定常性がどう現われるか興味あるところである．この点に本論の焦点を絞っている．

内容は次のように要約される．水平不透水層上の地山モデル中にく形単設空洞を設定し，境界水位が左右対称な流れを考え，空洞周辺の自由水面の非定常挙動と湧水量をヘル・ショウ実験と数値解析によって究明した．ヘル・ショウ実験装置は水平長さ1.05 m，高さ0.3 mであり，左右に貯留部をもち，オーバフロー槽により境界水位(0.15～0.25 m)をコントロールした．ヘル・ショウ実験における帯水層の油（動粘性係数：2.840×10^{-4} m²/s）の浸透係数は1.150×10^{-2} m/sであり，空洞寸法は0.025 mであった．この実験装置により，自由水面形は8 m/m写真で撮影し，湧水量の時間的変化は少容量のメスシリンダー中の貯留油位の経時変化を写真観測することから読み取って計った．

一方，数値解析は基礎式と自由表面条件を差分化したものを用いた．あらかじめ，数値解析手法の適用性をヘル・ショウ実験結果と比較して検討しておいて，実験では検討できない場合は数値計算によって究明する．

その結果，ヘル・ショウ実験によって，湧水量ハイドログラフは湧水初期に急激にてい減し，ある時点からてい減率が小さくなる特性をもつことが明らかになり，湧水レヂームを支配する変曲点の存在を提案することができた．しかし，その湧水レヂームの現われる理由が実験では解明できない．そこで，実験結果により数値解析法の適用性を吟味した後，数値解析によって空洞への湧水成分を3つに分解（空洞の直上からの流入，空洞左右壁面からの流入，および空洞底面からの成分）して，おのおのの湧水成分の全湧水への寄与程度を解明した．それより，湧水ハイドログラフに現われる変曲点は空洞上部から流入する湧水成分に依存することが判明した．このことは，本来空洞湧水をどうとらえればよいかという基本的に重要な現象の要を明示したものと考えられる．さらに，この湧水レヂームの違いは地山の境界条件水位が高いほど顕著に現われることが実験と理論の両面より明示された．さらに，重要となると思われる地山の異方性による湧水特性について，数値計算によって水平，鉛直透水係数比をいろいろ変えて検討し，地山の異方性と水面形の低下特性が明らかにされ，流れの場における流速ベクトルの分布も示された．

本論の結論としては，まず空洞への自由水面形と湧水が地山の異方性に関わる透水係数の空間分布に依存し，鉛直透水係数が大きいほど空洞直上の水位降下が早くなること，次いで，空洞直上に水面が到達する前後で湧水ハイドログラフに変曲点を生じ，湧水機構が変化することを実験と解析の両面よりつかんだことである．この2点は空洞の地下水流の解析を進める際に基本となる性質である．